INTRODUCTION TO KINETIC PLASMA THEORY WITH APPLICATIONS TO THE SOLAR WIND

Stefaan Poedts

CmPA / Dept. of Mathematics, KU Leuven, Leuven, Belgium
Institute of Physics, University of Maria Curie-Skłodowska, Lublin, Poland

Abstract

First, the place of kinetic theory among other mathematical models to describe plasma physics is discussed. Next, some basic kinetic concepts are introduced and the kinetic plasma equations are described. The use of these equations is then demonstrated considering electron plasma oscillations, a simple example of collective behaviour, and deriving a fundamental plasma parameter, viz. the plasma frequency, a fundamental plasma parameter. The a surprising fundamental phenomenon Landau damping is briefly discussed.

1 Introduction: theoretical models in plasma physics

Different mathematical models exist for different kinds of plasma processes. The model to be used or applied depends on the kind of phenomenon to be studied. Three kinds of theoretical description can be distinguished on the basis of the chosen approach [2]:

1. the theory of the motion of *individual charged particles* in given magnetic and electric fields; e.g. the motion of a charged, non-relativistic particle is described by

$$m\frac{d\mathbf{v}}{dt} = q(\mathbf{E} + \mathbf{v} \times \mathbf{B})\,, \tag{1}$$

   where $\mathbf{E}(\mathbf{r}, t)$ and $\mathbf{B}(\mathbf{r}, t)$ are given solutions of the Maxwell's equations, and one has to solve for the particle velocity $\mathbf{v}(\mathbf{r}, t)$. This model is useful to describe gyration of particles in a magnetic field and adiabatic invariants of this cyclotron motion, the magnetic mirror effect, drifts, etc. But plasmas usually contain a lot of particles, e.g. a large Corona Mass Ejection on the Sun involves up to 10^{30} particles, requiring a different model approach;

2. the *kinetic theory* of a such collections of charged particles, describing plasma behavior on a *microscopic scale* by means of particle distribution functions $f_{e,i}(\mathbf{r}, \mathbf{v}, t)$, the evolution of which is most generally described by the Boltzmann dissipative equation (see below). There exists an alternative Particle-In-Cell (PIC) approach, however, in which the particles are modelled as 'super particles' or 'particle clouds' which are accelerated by the forces (Lorentz, gravitational, etc.). This alternative approach will described in module KT-2;

3. the *fluid theory* (MHD), describing plasma behavior on a *macroscopic scale* in terms of averaged (over $\mathbf{v}$) functions of only $\mathbf{r}$ and t. The three basic steps to get from kinetic theory to the plasma model are discussed in the last section of this contribution.

Clearly, this is a rough division of model approaches and there exist combinations, like hybrid models with one or more species described in the fluid theory and other species described in kinetic theory. Here, we will focus on the kinetic plasma theory.

Why kinetic theory?

In the single particle orbit theory mentioned above, the interactions between the particles is ignored. This is a valid

assumption only when the density of the charged particles is low enough. Plasmas, however, exhibit *collective behaviour* because of the large amount of *interacting* particles involved. As a result, a statistical approach can be used to analyse its dynamics and this is precisely what kinetic plasma theory does. In this sense, the kinetic description of plasma is fundamental. The position of particles is known in phase space, the space of all possible values of position and momentum variables, making even the electron scale accessible.

Of particular importance are kinetic or micro-instabilities. These are short wavelength - high frequency modes of the system that may grow in amplitude when the charged particle species in a collisionless plasma posses a non-Maxwellian velocity distribution. In other words, these modes are driven unstable by the kinetic anisotropy of the plasma particles which provides a source of free energy. The velocity distributions (microstates) measured in-situ in space plasmas, for instance, often show departures from thermodynamic (Maxwellian) equilibrium in the form of temperature anisotropy, plasma flows or beams ('strahls'), suprathermal tails, etc. *These deviations from thermal equilibrium and the micro-instabilities they induce can be described only with a kinetic approach*.

Here, we will not elaborate on the derivation of the equation(s) describing the evolution of the plasma, which was introduced by Ludwig Boltzmann in 1872 and constitutes a vast amount of theoretical analysis (See, e.g. the comprehensive treatise by Balescu [3]), but merely exploit *the Boltzmann equation*, one of the end results of this work.

Closely following Goedbloed, Keppens, and Poedts [2], we will first introduce some basic kinetic concepts (Section 4) and consider a simple example of collective behaviour (Section 5), viz. electron plasma oscillations, and derive *the plasma frequency*, a fundamental plasma parameter. The (Landau) damping of these oscillations through kinetic effects is then discussed briefly in Section 5. It will also be discussed in modules KW-1 and KW-2 in this school. In module KT-2, numerical simulation models based on kinetic theory will be discussed and some of the impressive results will be demonstrated there.

2 Some basic plasma parameters

In Eq. (1) we did not specify the mass m and the charge q of the particles. Clearly, they correspond to either electrons ($m = m_e\,,\ q = -e$) or ions with mass number A and charge number Z (i.e. multiples of the proton mass and charge: $m = m_i = Am_p\,,\ q = Ze$). When we consider such a charged particle in a constant magnetic field in the z-direction, in the absence of an electric field: $\mathbf{B} = B\mathbf{e}_z\,,\ \mathbf{E} = 0\,,$ we can get some insight by performing two simple vector operations on Eq. (1). First project this equation $\mathbf{B}$ and using vector identities, we get that $v_\parallel = \text{const}$ because

$$m\frac{dv_\parallel}{dt} = 0\,. \tag{2}$$

When we project the same equation on $\mathbf{v}$, we get

$$\frac{d}{dt}(\tfrac{1}{2}mv^2) = 0 \ \rightarrow\ \tfrac{1}{2}mv^2 = \text{const}\,, \tag{3}$$

which in combination with (2) yields that also $v_\perp = \text{const.}$ because

$$\tfrac{1}{2}mv_\perp^2 = \text{const.} \tag{4}$$

Solving Eq. (1) more systematically, using $\mathbf{v} = d\mathbf{r}/dt = (\dot{x}, \dot{y}, \dot{z})$, we get two coupled differential equations describing the motion in the perpendicular plane:

$$\begin{aligned} \ddot{x} - \Omega\,\dot{y} &= 0\,, \\ \ddot{y} + \Omega\,\dot{x} &= 0\,, \end{aligned} \tag{5}$$

where

$$\Omega \equiv \frac{|q|B}{m}\,, \tag{6}$$

is *the gyro-* or *cyclotron frequency*.

We here do not elaborate on the derivation (see [2]), but the helical orbit consists of gyration (a periodic circular motion) $\perp \mathbf{B}$ about a *the guiding centre* and with a *the gyro-* or *cyclotron radius*

$$R \equiv \frac{v_\perp}{\Omega} = \text{const}\,, \tag{7}$$

and inertial motion $\parallel \mathbf{B}$. The magnetic field $\mathbf{B}$ thus determines the geometry of the plasma.

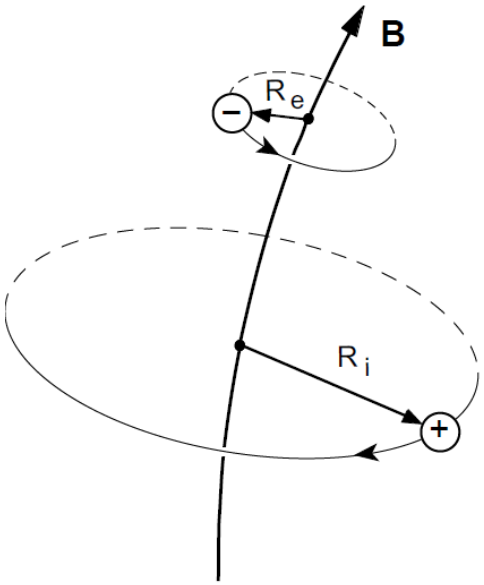

Figure 1: Gyration of electrons and ions in a magnetic field (source: [2]).

Remark that electrons and ions gyrate in opposite directions (Fig. 1). Due to their mass difference, their gyro-frequencies and gyro-radii are quite different:

$$\begin{aligned} \Omega_e &\equiv \frac{eB}{m_e} \quad \gg \quad \Omega_i \equiv \frac{ZeB}{m_i}\,, \\ R_e &\equiv \frac{v_{\perp,e}}{\Omega_e} \quad \ll \quad R_i \equiv \frac{v_{\perp,i}}{\Omega_i} \quad \text{(assuming } T_e \sim T_i\text{)}\,. \end{aligned} \tag{8}$$

Inserting a magnetic field $B = 3\,\mathrm{T}$ (= 30 kgauss), typical for tokamaks, and the values for e, m_e, and m_p, we find for the angular frequencies of protons and electrons

$$\begin{aligned} \Omega_e &= 5.3 \times 10^{11}\,\mathrm{rad\,s^{-1}} \quad \text{(i.e., a freq. of 84 GHz)}\,, \\ \Omega_i &= 2.9 \times 10^{8}\,\mathrm{rad\,s^{-1}} \quad \text{(i.e., a freq. of 46 MHz)}\,. \end{aligned} \tag{9}$$

Considering particles with thermal speed $v_\perp = v_{\rm th} \equiv \sqrt{2kT/m}$ we can estimate the gyro-radii. For electrons and protons at $\widetilde{T} = 10\,\mathrm{keV}$, i.e. $T_e = T_i = 1.16 \times 10^8\,\mathrm{K}$, we obtain

$$\begin{aligned} v_{\mathrm{th},e} &= 5.9 \times 10^{7}\,\mathrm{m\,s^{-1}} \quad \Rightarrow \quad R_e \approx 0.1\,\mathrm{mm}\,, \\ v_{\mathrm{th},i} &= 1.4 \times 10^{6}\,\mathrm{m\,s^{-1}} \quad \Rightarrow \quad R_i \approx 5\,\mathrm{mm}\,. \end{aligned} \tag{10}$$

Adding a constant background electric field perpendicular to the magnetic field, i.e. $\mathbf{B} = B\mathbf{e}_z$, $\mathbf{E} = E\mathbf{e}_y$, only slightly complicates the analysis. However, in this case the gyration is superposed with a constant 'drift' in $x-$direction. Hence, the perpendicular electric field results in the so-called $\mathbf{E} \times \mathbf{B}$ drift (see [2]).

3 Kinetic model equations

The equations of the kinetic model consist of equations for the particle distribution functions combined with Maxwell's equations (13) which determine the electric and magnetic fields $\mathbf{E}(\mathbf{r}, t)$ and $\mathbf{B}(\mathbf{r}, t)$.

3.1 The Boltzmann equation

Let us consider a plasma that consists of electrons and one kind of ions. Clearly, the information on the individuality of the particles is lost in the statistical description. However, the time-dependent *distribution functions* $f_\alpha(\mathbf{r}, \mathbf{v}, t)$ for the electrons and ions (α = e, i) contain relevant physical information on the plasma as a whole. The distribution functions express the density of the representation points of particles of type α in the six-dimensional *phase space* which is formed by the three position coordinates (x, y, z) and the three velocity coordinates (v_x, v_y, v_z) (see, e.g., Bittencourt [4]). In other words, $f_\alpha(\mathbf{r}, \mathbf{v}, t)\, d^3r\, d^3v$ represents the probable number of particles of type α in the six-dimensional volume element $d^3r\, d^3v$ centred at $(\mathbf{r}, \mathbf{v})$. We here assume that the total number of particles, $N_\alpha \equiv \iint f_\alpha d^3r\, d^3v$, is constant. This is, of course, not valid for plasmas that are in thermal and/or chemical non-equilibrium, like the partially-ionized plasmas in the lower solar atmosphere (photosphere and lower chromosphere) and thermonuclear plasmas in which fusion reactions create and annihilate particles. In such cases, more than two distribution functions are needed, e.g. also one for neutrals in the case of the solar photosphere, and the respective total number of particles will not be constant.

We now make a distinction between the motion of individual particles and the motion of a collection of their representative points in phase space, which is somehow similar to the motion of a swarm of bees (versus the motion of a particular bee in the swarm). The 'swarm' of representative points is described by the the distribution

function $f_\alpha(\mathbf{r},\mathbf{v},t)$, and its motion is given the *total* time derivative of f_α, using the chain rule we get:

$$\begin{aligned}\frac{\mathrm{d}f_\alpha}{\mathrm{d}t} &\equiv \frac{\partial f_\alpha}{\partial t}+\frac{\partial f_\alpha}{\partial \mathbf{r}}\cdot\frac{d\mathbf{r}}{dt}+\frac{\partial f_\alpha}{\partial \mathbf{v}}\cdot\frac{d\mathbf{v}}{dt} \\ &= \frac{\partial f_\alpha}{\partial t}+\mathbf{v}\cdot\frac{\partial f_\alpha}{\partial \mathbf{r}}+\frac{q_\alpha}{m_\alpha}\left(\mathbf{E}+\mathbf{v}\times\mathbf{B}\right)\cdot\frac{\partial f_\alpha}{\partial \mathbf{v}}, \end{aligned} \quad (11)$$

where Eq. (1) has been used inserted in the second line.

Here, the scalar products involving derivatives with respect to the vectors $\mathbf{r}$ and $\mathbf{v}$ simply denote sums over the products of the vector components, i.e. $\mathbf{v}\cdot\partial/\partial\mathbf{r} \equiv v_x\,\partial/\partial x + v_y\,\partial/\partial y + v_z\,\partial/\partial z$, and idem for the term with $\partial/\partial\mathbf{v}$. Notice also the subtle difference between $\mathrm{d}/\mathrm{d}t$ for the total time derivative and d/dt for ordinary time derivatives. Liouville's theorem ([6])states that, in the absence of binary interactions between particles, $\mathrm{d}f_\alpha/\mathrm{d}t = 0$, i.e. the density of representative points in phase space remains constant.

Clearly, the behaviour of a collection of particles only becomes interesting when these particles collide with each other, i.e. interact. In 1872, Ludwig Boltzmann derived an equation describing the time variation of the distribution functions of electrons and ions. This kinetic equation, called *the Boltzmann equation* reads:

$$\frac{\partial f_\alpha}{\partial t}+\mathbf{v}\cdot\frac{\partial f_\alpha}{\partial \mathbf{r}}+\frac{q_\alpha}{m_\alpha}\left(\mathbf{E}+\mathbf{v}\times\mathbf{B}\right)\cdot\frac{\partial f_\alpha}{\partial \mathbf{v}} = \left(\frac{\partial f_\alpha}{\partial t}\right)_{\mathrm{coll}}. \quad (12)$$

Note that here $\mathbf{E}(\mathbf{r},t)$ and $\mathbf{B}(\mathbf{r},t)$ consist of the contributions of the external fields plus that of the averaged internal fields originating from the long-range inter-particle interactions. The right-hand side represents the effect of an unspecified collision term which should model the short-range inter-particle interactions, or 'collisions'. These are the large-angle Coulomb collisions resulting from the cumulation of the many small-angle velocity changes. A first important objective of kinetic theory is to distinguish between different (long- and short-range) interactions and binary collisions and to determine on what ranges they are valid, yielding different forms of this collision term. One choice leads to the Landau collision integral (1936) [8]. And when only the accumulated effects of the small-angle collisions are taken into account, the above equation leads to the *Fokker–Planck equation*; and neglecting all collisions, i.e. setting the RHS equal to zero, leads to the *Vlasov equation* (1938) [20].

3.2 Maxwell's equations

In order to obtain a closed system of equations the Boltzmann equation (12) (or the Vlasov equation in case collisions can be ignored) for the distribution functions $f_\alpha(\mathbf{r},\mathbf{v},t)$, are combined with Maxwell's equations (13), determining the electric and magnetic fields $\mathbf{E}(\mathbf{r},t)$ and $\mathbf{B}(\mathbf{r},t)$, and providing expressions (14) for the charge and current density source terms $\tau(\mathbf{r},t)$ and $\mathbf{j}(\mathbf{r},t)$. In mksA units these equations are given by:

$$\begin{cases} \nabla\times\mathbf{E} = -\dfrac{\partial\mathbf{B}}{\partial t} & \text{(Faraday)}, \\ \nabla\times\mathbf{B} = \mu_0\mathbf{j}+\dfrac{1}{c^2}\dfrac{\partial\mathbf{E}}{\partial t} & \text{('Ampère')}, \; c^2=(\epsilon_0\mu_0)^{-1}, \\ \nabla\cdot\mathbf{E} \;= \dfrac{\tau}{\epsilon_0} & \text{(Poisson)}, \\ \nabla\cdot\mathbf{B} \;= 0 & \text{(no magnetic monopoles)}. \end{cases} \quad (13)$$

We have ignored polarisation and magnetisation effects, i.e. $\epsilon = \epsilon_0$ and $\mu = \mu_0$ so that $\mathbf{D} = \epsilon_0\mathbf{E}$ and $\mathbf{H} = (\mu_0)^{-1}\mathbf{B}$, since these effects are absorbed in the definitions of charge and current density:

$$\begin{cases} \tau = \sum_\alpha q_\alpha n_\alpha \\ \mathbf{j} = \sum_\alpha q_\alpha n_\alpha \mathbf{u}_\alpha \end{cases} \quad (\alpha = \text{e, i}). \quad (14)$$

Here, n_α and $\mathbf{u}_\alpha$ are the particle density and the macroscopic velocity of particles of type α.

The charge and current density source terms $\tau(\mathbf{r},t)$ and $\mathbf{j}(\mathbf{r},t)$ are related to the particle densities and the average velocities:

$$\begin{aligned} n_\alpha(\mathbf{r},t) &\equiv \int f_\alpha(\mathbf{r},\mathbf{v},t)\,d^3v\,, \\ \text{and}\;\; \tau(\mathbf{r},t) &\equiv \sum q_\alpha n_\alpha\,, \end{aligned} \quad (15)$$

$$\begin{aligned} \mathbf{u}_\alpha(\mathbf{r},t) &\equiv \frac{1}{n_\alpha(\mathbf{r},t)}\int \mathbf{v} f_\alpha(\mathbf{r},\mathbf{v},t)\,d^3v\,, \\ \text{and}\;\; \mathbf{j}(\mathbf{r},t) &\equiv \sum q_\alpha n_\alpha \mathbf{u}_\alpha\,. \end{aligned} \quad (16)$$

This completes the microscopic equations.

Solving these kinetic equations in seven dimensions (with the details of the single particle motions entering the collision integrals) is a formidable task, even with the help

of present-day supercomputers. Hence, whenever possible, i.e. when the physical phenomenon that is studied allows it, modelers will look for a macroscopic reduction. Here, however, we will stick to the kinetic equations and take up the challenge of solving them.

4 Moment reduction

Macroscopic equations, i.e. equations that do not involve details of velocity space any more can be obtained by expanding in a finite number of moments of the Boltzmann equation (12). These moments are obtained by first multiplying the equation with a function $\chi(\mathbf{v})$ and then integrating over velocity space. The function χ consists of powers of the velocity:

$$\chi(\mathbf{v}) = \begin{cases} 1, & \text{zeroth moment;} \\ \mathbf{v}, & \text{first moment;} \\ v^2, & \text{second moment;} \\ \dots & , \end{cases} \tag{17}$$

and the procedure is truncated after a finite number (5, 10, 20...) of such moments. Clearly, taking moments of the Boltsmann equation involves the moments of the distribution function itself. For instance, the zeroth moment is associated with the particle density $n_\alpha(\mathbf{r}, t)$ and the first moment is associated with the average velocity $\langle \mathbf{v} \rangle_\alpha \equiv \mathbf{u}_\alpha(\mathbf{r}, t)$, defined above. This expansion in moments clearly needs to be truncated in order to be practical. A popular truncation occurs already after the five moments (one scalar + one vector + one scalar) indicated explicitly in Eq. (17). This truncation is justified in the transport theory. Macroscopic variables $\langle g \rangle_\alpha(\mathbf{r}, t)$ generally appear as averages of some phase space function $g(\mathbf{r}, \mathbf{v}, t)$ over the velocity space, i.e.

$$\langle g \rangle_\alpha(\mathbf{r}, t) \equiv \frac{1}{n_\alpha(\mathbf{r}, t)} \int g(\mathbf{r}, \mathbf{v}, t)\, f_\alpha(\mathbf{r}, \mathbf{v}, t)\, d^3v\,. \tag{18}$$

Clearly, this definition assumes or requires that the distribution functions f_α decrease fast enough with $v \to \infty$ in order to yield a finite answer.

The systematic procedure of taking moments of the Boltzmann equations also involves the determination of the different moments of the collision term in the RHS. The collision operator

$$\left(\frac{\partial f_\alpha}{\partial t} \right)_{\text{coll}} \equiv C_\alpha\,, \tag{19}$$

represents evolution of f_α due to local collisions. It can be decomposed in contributions $C_{\alpha\beta}$ due to collisions of particles α (e.g. electrons) with particles β (i.e. electrons as well as ions):

$$C_\alpha = \sum_\beta C_{\alpha\beta}\,. \tag{20}$$

So, e.g. C_i is the sum of the intraspecies collision operator C_{ii}, which represents the effect of ion-ion collisions, and the interspecies collision operator C_{ie}, which represents the effect on the ions of ion-electron collisions. C_α is thus an operator which maps functions of velocity space, $f_i(\mathbf{v})$ and $f_e(\mathbf{v})$, to a function of velocity space, $C_\alpha(\mathbf{v})$.

The collision of course respect some constraints. For instance, in the absence of fusion reactions, there is *conservation of mass*, i.e. the total number of particles α at a certain position does not change by collisions with particles β:

$$\int C_{\alpha\beta}\, d^3v = 0\,. \tag{21}$$

In a similar way, *conservation of momentum* yields

$$\int \mathbf{v} C_{ii}\, d^3v = 0\,, \tag{22}$$

and

$$\int ||\mathbf{v}||^2 (C_i + C_e)\, d^3v = 0\,; \tag{23}$$

while *conservation of energy* yields

$$\int \mathbf{v} C_{ii}\, d^3v = 0\,, \tag{24}$$

and

$$\int ||\mathbf{v}||^2 (C_i + C_e)\, d^3v = 0\,. \tag{25}$$

More details of the derivation of these expressions and on the procedure in general can be found in Goedbloed, Keppens, and Poedts [2]. In order to give an idea of the procedure, we will here only derive the lowest moment equation, which describes mass conservation.

As mentioned above, the *zeroth moment* is obtained by integrating the Boltzmann equation (Eq. (12)) over velocity space. Doing this term by term, we get subsequently:

$$\int \frac{\partial f_\alpha}{\partial t}\, d^3v \;=\; \frac{\partial n_\alpha}{\partial t} \qquad \text{(def. (15))}\,,$$

$$\int \mathbf{v}\cdot\frac{\partial f_\alpha}{\partial \mathbf{r}}\, d^3v \;=\; \nabla\cdot(n_\alpha \mathbf{u}_\alpha) \text{ (def. (16))}\,,$$

$$\int \frac{q_\alpha}{m_\alpha}\,(\mathbf{E}+\mathbf{v}\times\mathbf{B})\cdot\frac{\partial f_\alpha}{\partial \mathbf{v}}\, d^3v \;=\; 0 \quad \text{(int. by parts)},$$

$$\int C_\alpha\, d^3v \;=\; 0 \quad \text{(summing Eq. (21))}\,.$$

The continuity equation for particles of species α is obtained by adding these four expressions, yielding

$$\frac{\partial n_\alpha}{\partial t} + \nabla\cdot(n_\alpha \mathbf{u}_\alpha) = 0\,. \tag{26}$$

Similarly, the *first moment* of the Boltzmann equation is obtained by multiplying it with $m_\alpha \mathbf{v}$ and integrating this expression over the velocities. This yields *the momentum equation*:

$$\frac{\partial}{\partial t}\,(n_\alpha m_\alpha \mathbf{u}_\alpha) + \nabla\cdot\Big(n_\alpha m_\alpha \langle \mathbf{v}\mathbf{v}\rangle_\alpha\Big) - q_\alpha n_\alpha(\mathbf{E}+\mathbf{u}_\alpha\times\mathbf{B}) = \int C_{\alpha\beta}\, m_\alpha \mathbf{v}\, d^3v\,. \tag{27}$$

The *scalar second moment* of Eq. (12) is then obtained by multiplying with $\frac{1}{2}m_\alpha v^2$ and integrating over velocity space. This yields *the energy equation*:

$$\frac{\partial}{\partial t}\Big(n_\alpha \tfrac{1}{2} m_\alpha \langle v^2\rangle_\alpha\Big) + \nabla\cdot\Big(n_\alpha \tfrac{1}{2} m_\alpha \langle v^2 \mathbf{v}\rangle_\alpha\Big) - q_\alpha n_\alpha \mathbf{E}\cdot\mathbf{u}_\alpha = \int C_{\alpha\beta}\, \tfrac{1}{2} m_\alpha v^2\, d^3v\,. \tag{28}$$

See [2] for the explicit steps in the derivation of these equations.

This chain of moment equations can be continued indefinitely. Notice that each moment introduces a new unknown whose temporal evolution is described by the next moment of the Boltzmann equation. However, the infinite chain must be truncated to be useful. In fluid theories truncation is just after the above five moments: the continuity equation (26) (scalar), the momentum equation (27) (vector), and the energy equation (28) (scalar), by making additional assumptions. In (very) broad outlines, the procedure can be summarized as follows:

(a) First, split the particle velocity $\mathbf{v}$ into an average part $\mathbf{u}_\alpha$ and a random part $\tilde{\mathbf{v}}_\alpha$, i.e.

$$\tilde{\mathbf{v}}_\alpha \equiv \mathbf{v} - \mathbf{u}_\alpha\,, \quad \text{where } \langle\tilde{\mathbf{v}}_\alpha\rangle = 0\,. \tag{29}$$

In this way *thermal quantities* can be defined, like

$$T_\alpha(\mathbf{r},t) \equiv \frac{m_\alpha}{3k}\,\langle \tilde{v}_\alpha^2\rangle \qquad \textit{(temperature)}\,, \tag{30}$$

$$\mathbf{P}_\alpha(\mathbf{r},t) \equiv n_\alpha m_\alpha\,\langle\tilde{\mathbf{v}}_\alpha\tilde{\mathbf{v}}_\alpha\rangle = p_\alpha \mathbf{I} + \boldsymbol{\pi}_\alpha\,,$$
$$p_\alpha \equiv n_\alpha k T_\alpha \qquad \textit{(stress tensor)}, \tag{31}$$

$$\mathbf{h}_\alpha(\mathbf{r},t) \equiv \tfrac{1}{2} n_\alpha m_\alpha\,\langle \tilde{v}_\alpha^2 \tilde{\mathbf{v}}_\alpha\rangle \qquad \textit{(heat flow)}\,, \tag{32}$$

$$\mathbf{R}_\alpha(\mathbf{r},t) \equiv m_\alpha \int C_{\alpha\beta}\tilde{\mathbf{v}}_\alpha d^3v \;\textit{(momentum transfer)}, \tag{33}$$

$$Q_\alpha(\mathbf{r},t) \equiv \tfrac{1}{2} m_\alpha \int C_{\alpha\beta}\,\tilde{v}_\alpha^2\, d^3v \quad \textit{(heat transfer)}\,. \tag{34}$$

Note that in this notation $\mathbf{I}$ is the unit tensor, i.e. $\boldsymbol{\pi}_\alpha$ represents the off-diagonal terms of the pressure tensor $\mathbf{P}$. For instance, the *Maxwell distribution* for thermal equilibrium:

$$f_\alpha^0(\mathbf{r},\mathbf{v},t) = n_\alpha \left(\frac{m_\alpha}{2\pi k T_\alpha}\right)^{3/2} \exp\left(-\frac{m_\alpha \tilde{v}_\alpha^2}{2kT_\alpha}\right), \tag{35}$$

is consistent with these definitions and makes the LHS of the Boltzmann equation (12) vanish. This means that the collision term on the RHS should vanish too, i.e. when the two distributions have equal average velocities ($\mathbf{u}_e = \mathbf{u}_i$) and temperatures ($T_e = T_i$). The deviations from this thermal equilibrium and the way in which collisions cause relaxation to thermal equilibrium, is what plasma kinetic theory is concerned with (Braginskii [5]).

(b) The temperature evolution equation is then transformed into a pressure evolution equation by introducing the ratio of specific heats, $\gamma \equiv C_p/C_v = 5/3$. The resulting equations for n_α, $\mathbf{u}_\alpha$, and p_α then appear rather macroscopic, but still hide unsolved kinetic dependencies involving higher order moments and variables which involve the unspecified collision operator.

(c) The obtained truncated set of moment equations is then finally closed by exploiting the transport coefficients derived by *transport theory* (Braginskii [5], Balescu [3]), which concerns the deviations from local thermodynamic equilibrium, expressed by Eq. (35). In this theory the distribution functions are developed in powers of a small parameter measuring these deviations. This results in *transport coefficients*, determining relations between the thermal quantities defined in Eqs. (30)–(34) and the gradients of the macroscopic quantities. The second objective of kinetic theory is to provide these coefficients, which is again a formidable task.

Following [2], we will now present an application of the two-fluid description (Section 5). It will be highly simplified in the sense that most of the complicated terms discussed above do not occur. Yet, this simple application illustrates a very important basic physical mechanism at work, namely collective electrostatic oscillations. After that, we will return to the kinetic description in terms of distribution functions and discuss how velocity space effects lead to Landau damping, a surprising kinetic phenomenon (Section 6).

5 Collective phenomena: plasma oscillations

Chen [7] defines a plasma as *a quasi-neutral gas of charged and neutral particles which exhibits collective behaviour*. The typical size of a region in the plasma over which charge imbalance due to thermal fluctuations may occur, is the *Debye length*. In the present section, we will extend these electric field concepts. We will first study perturbations of quasi-neutrality in a cold plasma by typical *plasma oscillations* which are called Langmuir waves (1929) [1]. We then study how these oscillations are affected by finite temperatures; first by including a finite pressure, next by taking into account velocity space effects by applying the kinetic equations, which will lead to the concept of *Landau damping*.

[1] named after the author who also introduced the term 'plasma' in 1923

5.1 Cold plasma oscillations

We start by considering a highly simplified case, viz. that of a cold plasma in the absence of a magnetic field ($\mathbf{B} = 0$). In other words, all thermal effects are neglected ($\mathbf{P}_\alpha$, $\mathbf{h}_\alpha$, $\mathbf{R}_\alpha$, and Q_α vanish). As a result, all the complicated terms in the equations of motion vanish and the energy equations can be dropped. For cold plasma oscillations we thus just need to consider the continuity equations,

$$\frac{\partial n_\alpha}{\partial t} + \nabla \cdot (n_\alpha \mathbf{u}_\alpha) = 0 \qquad (\alpha = e, i)\,, \tag{36}$$

and the simplified ($\mathbf{B} = 0$) momentum equations,

$$m_\alpha \Big(\frac{\partial \mathbf{u}_\alpha}{\partial t} + \mathbf{u}_\alpha \cdot \nabla \mathbf{u}_\alpha \Big) = q_\alpha \, \mathbf{E} \qquad (\alpha = e, i)\,. \tag{37}$$

The *Poisson equation* (13)(c) then enables us to determine the electric field in a self-consist manner, where *the charge density* is obtained from Eq. (14)(a):

$$\nabla \cdot \mathbf{E} = \frac{\tau}{\epsilon_0} = \frac{e}{\epsilon_0} \left(Z n_i - n_e \right). \tag{38}$$

Remark that these equations form a complete set for the variables $n_{e,i}(\mathbf{r}, t)$, $\mathbf{u}_{e,i}(\mathbf{r}, t)$, and $\mathbf{E}(\mathbf{r}, t)$ which describe the problem of electrostatic oscillations.

One of the most fundamental properties of plasmas is that they maintain approximate charge neutrality. As a matter of fact, charge imbalances on a macroscopic scale L would create huge electric fields ($E \sim \tau L/\epsilon_0$) which would accelerate the electrons and thus neutralise these imbalances extremely fast. As a result, the plasma maintains almost perfect charge neutrality.

Charge imbalances do occur, however, on a finer time and length scale, viz. in the form of typical oscillations. For these plasma oscillations, we can consider the heavy ions ($m_i \gg m_e$) as a fixed ($\mathbf{u}_i = 0$) neutralising background in which only the light electrons move ($\mathbf{u}_e \neq 0$). When a small region inside the plasma is then perturbed, by displacing the electrons in that region, the charge neutrality is disturbed ($n_e \neq Z n_i$). The problem is then completely determined by the electron variables (the two ion equations (36) and (37) for $\alpha = i$ may be dropped):

$$\begin{aligned} n_e &\approx n_0 + n_1(\mathbf{r}, t)\,, \\ \mathbf{u}_e &\approx \qquad\quad \mathbf{u}_1(\mathbf{r}, t)\,, \end{aligned} \tag{39}$$

whereas the ion variables simplify to

$$n_i \approx n_0/Z = \text{const}\,, \qquad \mathbf{u}_i \approx 0\,. \tag{40}$$

Here, the subscripts 0 and 1 refer to the constant background and the (small) perturbations, respectively. The small density perturbation $|n_1(\mathbf{r},t)| \ll n_0$ occurs in a small region of the plasma. We can thus *linearize* the equations, i.e. we can neglect terms involving products of perturbations since these are much smaller than the linear terms. As a result, the small electric field $\mathbf{E}_1$ that is created is proportional to n_1 and creates a small electron flow velocity $\mathbf{u}_1$, which is also proportional to n_1.

A complete set of equations is thus obtained, consisting of the linearized electron density equation (36), the momentum equation (37) (both with $\alpha = e$), and the Poisson equation (38):

$$\begin{aligned} &\frac{\partial n_1}{\partial t} + n_0 \nabla\cdot\mathbf{u}_1 = 0\,,\\ &m_e \frac{\partial \mathbf{u}_1}{\partial t} = -e\mathbf{E}_1\,,\\ &\nabla\cdot\mathbf{E}_1 = \frac{\tau_1}{\epsilon_0} = -\frac{e}{\epsilon_0}\,n_1\,. \end{aligned} \tag{41}$$

Eliminating $\mathbf{u}_1$ and $\mathbf{E}_1$ then yields a single wave equation for n_1:

$$\frac{\partial^2 n_1}{\partial t^2} = -n_0\nabla\cdot\frac{\partial \mathbf{u}_1}{\partial t} = \frac{n_0 e}{m_e}\nabla\cdot\mathbf{E}_1 = -\frac{n_0 e^2}{\epsilon_0 m_e}\,n_1\,. \tag{42}$$

5.2 Plasma frequency and Debye length

The solutions of the wave equation (42) can be written in the form $n_1(\mathbf{r},t) = \hat{n}_1(\mathbf{r})\exp(-\mathrm{i}\omega t)$. They represent *plasma oscillations*, which are electron density oscillations with a characteristic frequency, called *the electron plasma frequency*:

$$\omega = \pm\omega_{pe}\,, \quad \omega_{pe} \equiv \sqrt{\frac{n_0 e^2}{\epsilon_0 m_e}}\,. \tag{43}$$

This frequency is one of the fundamental parameters of a plasma and is usually very high (because m_e is very small). It provides a diagnostic for the determination of the plasma density since it depends only the plasma density. In tokamak plasmas, a typical density $n_0 = 10^{20}\,\mathrm{m}^{-3}$ gives

$$\omega_{pe} = 5.7\times10^{11}\,\mathrm{rad\,s^{-1}} \quad \text{(i.e. 91 GHz)}\,,$$

which is of the same order of magnitude as the electron cyclotron frequency for tokamaks with very strong magnetic fields ($B \sim 3\,\mathrm{T}$).

Remark that in cold plasma theory the spatial form of the amplitude $\hat{n}_1(\mathbf{r})$ of the plasma oscillations is not determined. This is different for 'warm' plasmas, where deviations from charge neutrality due to thermal fluctuations occur in small regions of a size of the order of the *Debye length*

$$\lambda_\mathrm{D} \equiv \sqrt{\frac{\epsilon_0 k_\mathrm{B} T_e}{n_0 e^2}} = \frac{v_{\mathrm{th},e}}{\sqrt{2}\,\omega_{pe}}\,. \tag{44}$$

Note that we here indicate the Boltzmann constant with a subscript, k_B, to distinguish it from the wave number k of the waves that now enters the analysis. For thermonuclear plasmas, with $\widetilde{T} = 10\,\mathrm{keV}$, $v_{\mathrm{th},e} = 5.9\times10^7\,\mathrm{m\,s^{-1}}$, $\omega_{pe} = 5.7\times10^{11}\,\mathrm{rad\,s^{-1}}$ gives

$$\lambda_\mathrm{D} = 7.4\times10^{-5}\,\mathrm{m} \approx 0.07\,\mathrm{mm}\,,$$

i.e. the Debye length is of the order of the electron gyroradius R_e.

5.3 (Finite pressure) Plasma oscillations

In warm plasmas, the frequency of the plasma oscillations becomes dependent on the wavelength because of the above-mentioned thermal fluctuations. The thermal contributions may be computed by means of the two-fluid equations for an unmagnetised plasma ($\mathbf{B} = 0$), assuming an isotropic pressure and neglecting heat transport and collisions. Assuming immobile ions again and linearising these equations for the electrons, like we did before for a cold plasma, we now get a modified eigenvalue problem where the pressure $p_0 = n_0 k_\mathrm{B} T_0$, i.e. the temperature, of the background plasma enters:

$$\frac{\partial n_1}{\partial t} + n_0\nabla\cdot\mathbf{u}_1 = 0\,, \tag{45}$$

$$n_0 m_e \frac{\partial \mathbf{u}_1}{\partial t} + \nabla p_1 = -e n_0 \mathbf{E}_1\,, \tag{46}$$

$$\frac{\partial p_1}{\partial t} + \gamma p_0 \nabla\cdot\mathbf{u}_1 = 0\,, \tag{47}$$

$$\nabla\cdot\mathbf{E}_1 = -\frac{e}{\epsilon_0}\,n_1\,. \tag{48}$$

Assuming plane waves in the x-direction, and ignoring spatial dependencies in the y- and z-directions,

$$n_1(x,t) = \hat{n}_1 \mathrm{e}^{\mathrm{i}(kx-\omega t)}, \tag{49}$$

(and similar expressions for $\mathbf{u}_1$, p_1, $\mathbf{E}_1$), the gradients $\nabla \to \mathrm{i}k\mathbf{e}_x$ and the time derivatives $\partial/\partial t \to -\mathrm{i}\omega$, so that Eqs. (45)–(48) become an algebraic system of equations for the amplitudes $\hat{n}_1$, $\hat{\mathbf{u}}_1$, $\hat{p}_1$, and $\hat{\mathbf{E}}_1$. The dispersion equation is obtained from the determinant and reads

$$\omega^2 = \omega_{pe}^2(1+\gamma k^2 \lambda_{\mathrm{D}}^2)\,. \tag{50}$$

Notice that here, since the oscillations are one-dimensional, we should exploit the value $\gamma = 3$ (see Chen [7], Chapter 4). Remark that the (c)old result (43) is recovered for long wavelengths, where $k^2\lambda_{\mathrm{D}}^2 \ll 1$, but there is a large effect now on the oscillations for wavelengths of the order of or smaller than the Debye length. However, this thermal correction of the dependence of ω on k turns out to be incomplete as misses the damping obtained in the proper kinetic derivation. We will discuss this briefly in the next section.

6 Collective phenomena: Landau damping

Following Goedbloed, Keppens, and Poedts [2], we remark that a more refined analysis of longitudinal plasma oscillations for 'warm' plasmas should take velocity space effects into account, exploiting the Vlasov, or *collisionless* Boltzmann, equation (12) (with vanishing RHS) for the perturbations $f_1(\mathbf{r},\mathbf{v},t)$ of the electron distribution function. Considering again plane wave solutions $\sim \exp \mathrm{i}(\mathbf{k}\cdot\mathbf{r}-\omega t)$, one immediately runs into a mathematical problem:

$$\frac{\partial f_1}{\partial t} + \mathbf{v}\cdot\frac{\partial f_1}{\partial \mathbf{r}} = -\mathrm{i}(\omega - \mathbf{k}\cdot\mathbf{v})\, f_1 = \frac{e}{m_e}\mathbf{E}_1 \cdot \frac{\partial f_0}{\partial \mathbf{v}}\,, \tag{51}$$

so that inversion of the operator $\partial/\partial t + \mathbf{v}\cdot\partial/\partial\mathbf{r}$, to express f_1 in terms of $\mathbf{E}_1$, leads to singularities for every $\omega - \mathbf{k}\cdot\mathbf{v} = 0$. Landau (1946) [9] performed a proper treatment of the related initial value problem, and showed that these singularities give rise to damping of the plasma oscillations, now called *Landau damping*. Since there is no dissipation as we are considering a purely collisionless medium here, this is a surprising phenomenon! Twenty years later, Malmberg and Wharton [12] verified the phenomenon of Landau damping experimentally. In fact, later (1968) these authors also demonstrated that the information contained in the initial signal may be recovered by means of plasma wave echos, i.e. it is not lost [13].

Van Kampen (1955) [18, 19] considered a complementary approach to the electrostatic plasma oscillations by means of a normal mode analysis. In this approach, the singularities $\omega - \mathbf{k}\cdot\mathbf{v} = 0$ lead to a continuous spectrum of singular, δ-function type, modes (the Van Kampen modes), which constitute a complete set of 'improper' eigenmodes for this system. Damping occurs because of *phase mixing*, a package of those modes rapidly loses its spatial phase coherence.

6.1 Landau's solution of the initial value problem

For a more careful analysis, which is beyond the level of this introductory chapter, we refer to Goedbloed, Keppens, and Poedts [2].

Landau's careful study of the initial value problem of electrostatic plasma oscillations shows that there is an important contribution of the singularities $v = v_{\mathrm{ph}} \equiv \omega/k$ where the particles are in resonance with the phase velocity of the waves. For a Maxwell distribution, the solution of the dispersion equation (obtained by Landau) for long wavelengths ($k\lambda_{\mathrm{D}} \ll 1$) is given by

$$\omega \approx \omega_{pe}\Big\{1+\tfrac{3}{2}k^2\lambda_{\mathrm{D}}^2 - \mathrm{i}\sqrt{\tfrac{\pi}{8}}\,(k\lambda_{\mathrm{D}})^{-3}\, e^{-\frac{1}{2}(k\lambda_{\mathrm{D}})^{-2}-\frac{3}{2}}\Big\}\,, \tag{52}$$

where the imaginary part represents *damping of the waves*. For long wavelengths, this damping is exponentially small. For short wavelengths ($k\lambda_{\mathrm{D}} \sim 1$), the damping becomes very strong so that wave motion with wavelengths smaller than the Debye length becomes impossible.

7 Kinetic processes in the solar wind

7.1 Proton and electron distribution data

Kinetic theory is necessary to explain observations of the velocity distribution functions of protons and electrons at 1 au (about the average distance from the Sun to the Earth, $149\,597\,871$ kilometers). Old Helios observations[14] of proton distributions show a variety of temperature anisotropies. Some examples are given in Fig. 2 which shows cuts through the velocity distribution functions (VDFs) in the ecliptic plane. The left column shows the proton distribution in the slow wind (with typical velocity of 300-350 km/s) at different distances from the Sun. Helios went all the way to 0.3 au[2]. The right column shows the same for the fast solar wind (typically 700 km/s) and the middle column corresponds to the intermediate wind. The dashed lines represent the local magnetic field.

The coloured isocontours of the VDFs displayed in Fig. 2 show that they come in a variety of shapes. The proton distribution is highly anisotropic: the perpendicular temperature $T_\perp$ is higher than the parallel temperature $T_\parallel$, which is most apparent in the proton distributions at low heliospheric distances and in the intermediate and fast solar wind (middle and RHS bottom plots in Fig. 2. Moreover, the proton distribution has a core part (red and orange contours) and a slightly drifting suprathermal 'halo' part (the blue contours). Some distributions are deformed by the asymmetric (magnetic field aligned) beam or 'strahl', which is also suprathermal and most apparent in the intermediate wind distribution at 0.39 au. The electron distributions (not shown here) are similar although they have a less anisotropic core. They also have a suprathermal halo and the electron distribution s are also deformed by an asymmetric (field aligned) strahl.

These features of the observed proton and electron distribution functions in the solar wind can be described with combinations non-Maxwellian and kappa distribution functions and explained by kinetic theory. In fact, the observed temperature anisotropy is much higher than theory predicts, so there must be some additional perpendicular heating going on to explain this.

[2]Actually, Helios A (launched in December 1974) went as close to the Sun as 0.31 au and Helios B (launched in January 1976) even to 0.29 au ($= 43\,432$ million km).

7.2 Modelling the velocity distribution functions

The complicated VDFs shown in Fig. 2 are modelled in (linear) theory using distribution functions with a (bi-)Maxwellian quasi-thermal core, like

$$f_{\rm core}(v_\parallel, v_\perp) = n_c C_M \exp\left[-\frac{v_\parallel^2}{w_\parallel^2} - \frac{v_\perp^2}{w_\perp^2}\right], \qquad (53)$$

while the non-thermal component is described by different Kappa distribution functions. The suprathermal halo, for instance, can be modelled by a bi-Kappa distribution function:

$$f_{\rm halo}(v_\parallel, v_\perp) = n_h C_\kappa \left[-\frac{v_\parallel^2}{\kappa\theta_\parallel^2} - \frac{v_\perp^2}{\kappa\theta_\perp^2}\right]^{-\kappa-1}, \qquad (54)$$

while the suprathermal, asymmetric (magnetically field-aligned) strahl or beam can be modelled by a drifting Kappa distribution function:

$$f_{\rm strahl}(v_\parallel, v_\perp) = n_s C'_\kappa \left[-\frac{(v_\parallel - V_0)^2}{\kappa'\theta^2} - \frac{v_\perp^2}{\kappa'\theta^2}\right]^{-\kappa'-1}. \qquad (55)$$

An example of such a complicated VDF with a bi-Maxwellian core, a bi-kappa halo, and a drifting Kappa strahl, is shown in Fig. 3. So the non-thermal part is split in a halo and a strahl both modelled by kappa distributions.

7.3 Occurrence rates of the temperature anisotropy

A summary of the solar wind distribution at 1 au (Earth orbit) is given in Figures 4 (core + halo protons) and 5 (core electrons). These figures contain millions of data points from different spacecraft (mostly WIND) over decades summarised in 2D plots. They have been produced by Peter Yoon who combined data from different sources[17, 1, 15, 10, 11]. At 1 au most protons are broadly distributed near quasi-isotropic conditions (the red dot in the meddle). The proton data distribution boundaries have a strange shape. It turns out that this outer boundary can be explained by kinetic processes, namely instabilities and collisions.

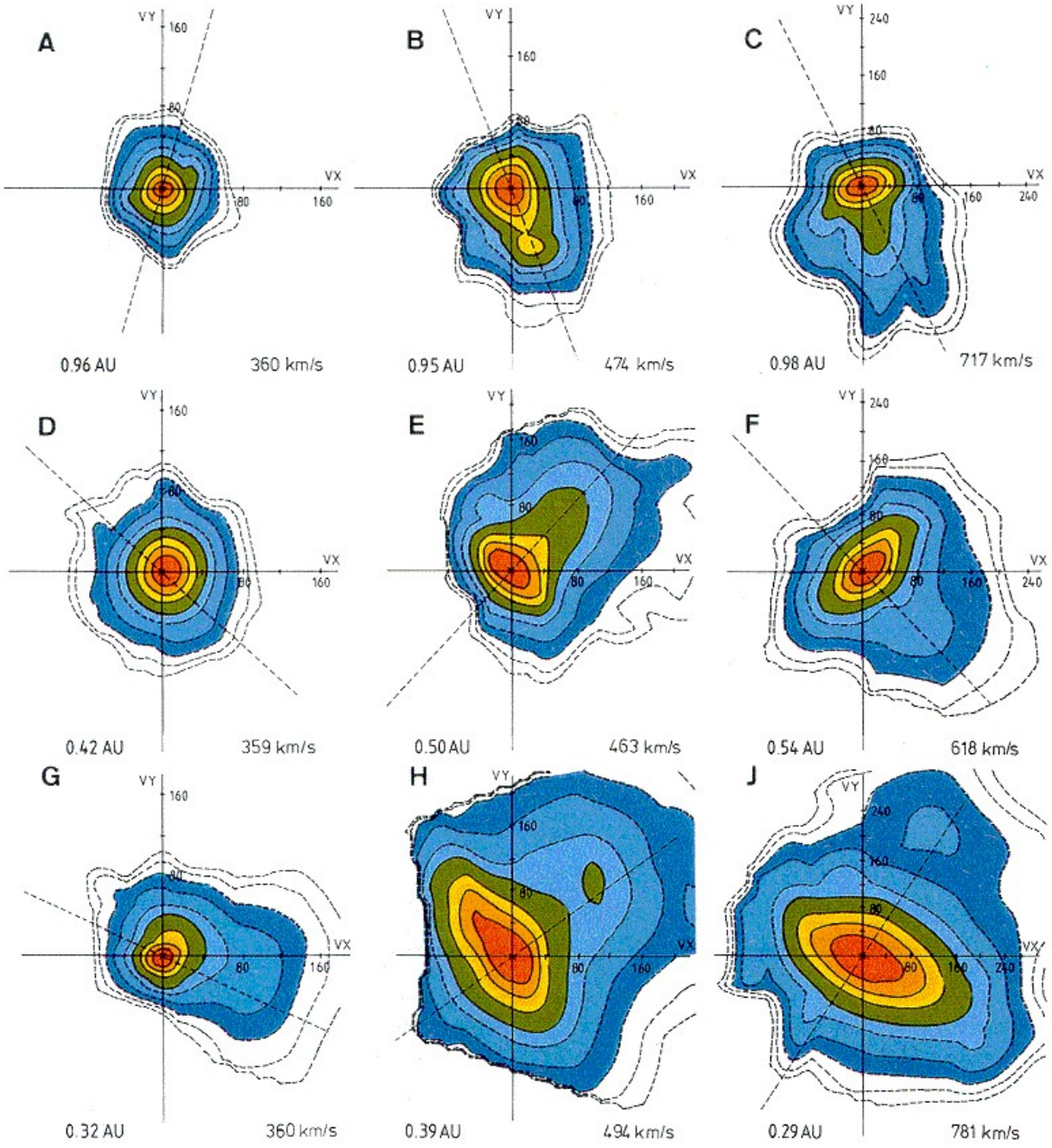

Figure 2: Proton velocity distribution functions in the solar wind near the perihelion of the Helios spacecraft and farther out. The VDFs have different shapes. Some are isotropic, others are anisotropic in perpendicular temperature and some are asymmetric, showing a magnetic field-aligned beam of 'strahl'. From Marsch[14]

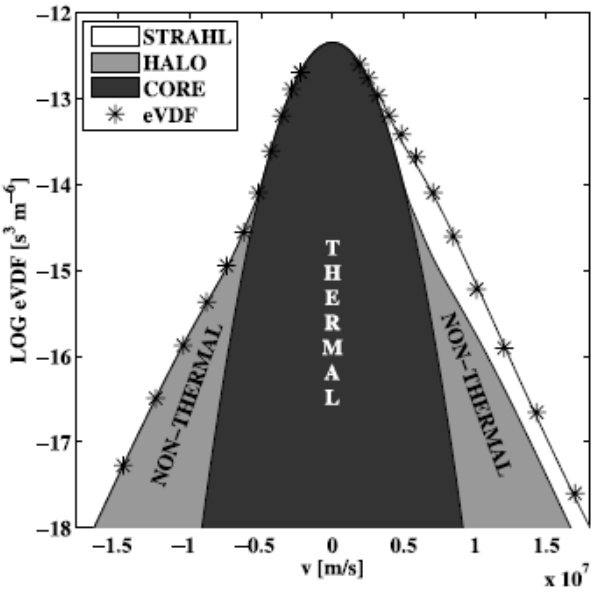

Figure 3: The modified model used for electron distributions by Štverák et al.[17] contains a thermal core and a non-thermal part consisting of a halo and a strahl, which gives a better estimate of their relative densities.

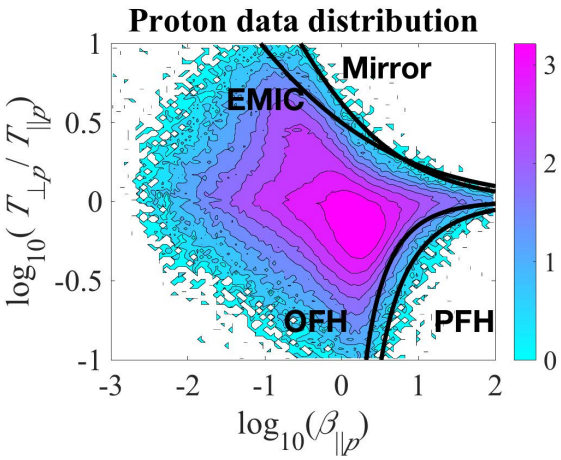

Figure 4: Log-log plot of the occurrence rates of the proton temperature anisotropy $T_{\perp p}/T_{\|p}$ versus the parallel plasma beta $\beta_{\|p}$ for the entire (core + halo) proton population in the solar wind at 1 au (Earth orbit). The over-plotted curves represent the marginal stability threshold for the indicated instabilities. Credit: Peter Yoon.

The core of the electron data distribution shown in Fig. 5 shows a similar behaviour. The halo electron data distribution, not shown here, is somewhat less anisotropic.

7.4 Kinetic processes behind the temperature anisotropy

The proton and electron data distributions shown in Figs. 4 and 5 show strange outer boundaries to the right. These can be explained by a number of marginal kinetic instability thresholds. When $T_\perp > T_\|$, there are electromagnetic electron cyclotron (whistler) instability (EMEC) and electromagnetic ion (proton) cyclotron instability (EMIC) and mirror instabilities with their marginal thresholds indicated in Figs. 4 and 5 (black lines at upper right boundaries). And when $T_\| > T_\perp$, there are the parallel proton (PFH) and electron (EFH) firehose and oblique proton firehose (OFH) instability thresholds, all indicated in Figs. 4 and 5 (black lines in lower right boundaries). The firehose modes and mirror modes are basically fluid modes, but kinetic theory provides a better

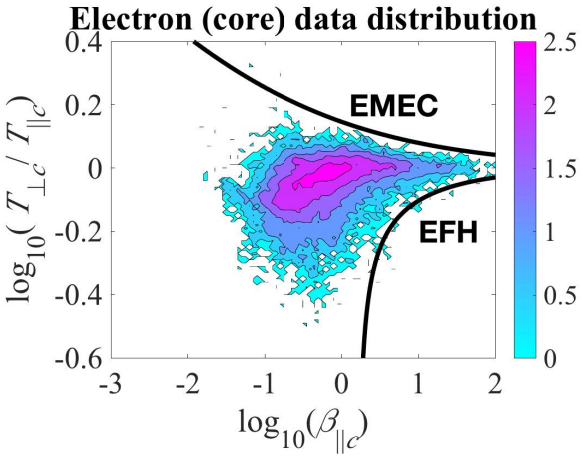

Figure 5: Log-log plot of the occurrence rates of the electron temperature anisotropy $T_{\perp e}/T_{\|e}$ versus the parallel plasma beta $\beta_{\|e}$ for the core electron population in the solar wind at 1 au. The over-plotted curves represent the marginal stability threshold for the EMEC nd EFH instabilities. Credit: Peter Yoon.

description of these instabilities. EMIC is clearly a kinetic instability.

The same EMEC/whistler and EFH marginal stability thresholds define the right outer boundaries of the hot (halo) component of the electron data distribution. So the thresholds of these instabilities determine the right outer boundaries of the distributions mentioned before from marginal stability conditions, which is linear theory.

7.5 Quasi-linear theory

However, linear theory does not take into account the dynamics, the changes of the background inhomogeneity, as it assumes it is in equilibrium. To take the background dynamics into account a nonlinear theory is needed. Quasi-linear theory describes the slow evolution of the distribution functions and their relaxation back to a marginally stable state. Quasi-linear theory is limited solely to determining how the distribution functions relax and, therefore, the simplest nonlinear theory. But it partially explains the observed outer boundaries. According to quasi-linear theory, $T_{\parallel}$ and $T_{\perp}$ evolve due to these instabilities and so do the magnetic field perturbations. Quasi-linear theory yields a dispersion relation for parallel propagation, so EMIC [16].

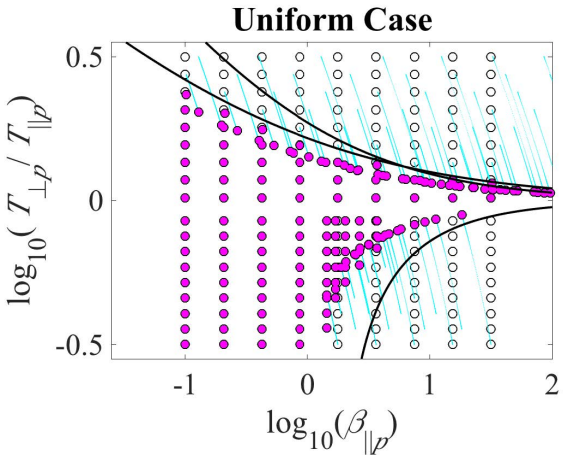

Figure 6: Log-log plot of the proton temperature anisotropy $T_{\perp p}/T_{\parallel p}$ versus the parallel plasma beta $\beta_{\parallel p}$ of the results obtained by solving the equations from quasi-linear theory. Credit: Peter Yoon.

Solving the equations of quasi-linear theory[16], results in the plot shown in Fig. 6 created by Peter Yoon. The open white dots are some hypothetical initial conditions. When unstable, they move to the marginal stability threshold and are coloured when they reach their final, marginally stable position. When the initial conditions are stable, they stay in place and are coloured too. The outer boundaries on the RHS are more or less reproduced like this, which you can see on the right and by comparing this figure with Fig. 4.

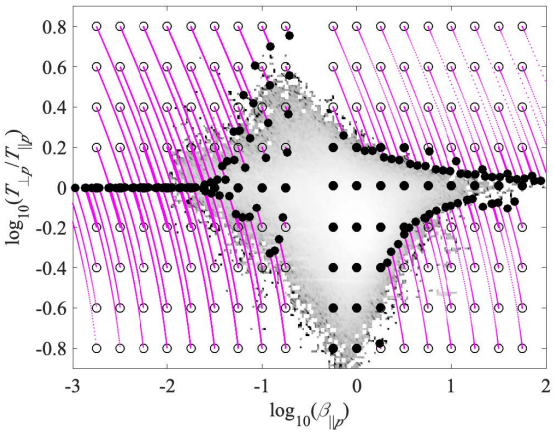

Figure 7: $T_{\perp p}/T_{\parallel p}$ versus $\beta_{\parallel p}$ log-log plot of the results obtained by solving the relaxation equations for binary collisions combined with the equations from quasi-linear theory from Fig. 6. Credit: Peter Yoon.

For explaining the boundaries to the left another kinetic process is needed. Indeed, when there are no instabilities operative, one has to bring in some other kinetic relaxation process, namely binary collisions. The relaxation equations for binary collisions[16] can be solved/relaxed as before. The result is seen in Fig. 7, which is again created by Peter Yoon and which is a combined figure showing the effect of collisions and instabilities at the same time. The white dots (representing initial conditions) move along the magenta lines and all settle down, according to the collision relaxation equations, and they are coloured black when they do. Hence, combining the quasi-linear equations with the relaxation equations results in Fig. 7 which can be directly compared to Fig. 4.

The points to the upper right are EMIC unstable and move down close to EMIC marginal stability threshold. Points to the lower RHS are firehose unstable and move up, lining up along the firehose marginal stability threshold. All the points to the left, on the other hand, are not unstable but they respond to collisions. They also move and line up. The result nicely fits the outer boundaries of the proton data distribution on the left as seen by comparing this figure to the data (Fig. 4): a nice example of how you can involve kinetic processes to explain observations.

8 From kinetic theory to fluid description

In this section we come back to the text of Goedbloed, Keppens, and Poedts [2]. We have seen that kinetic theory involves the detailed evolution of the distribution functions on very short length and time scales, such as the Debye length $\lambda_{\rm D}$ and the plasma frequency ω_{pe}. The development of the fluid picture of plasmas from the kinetic theory involves three major steps, illustrated in Fig. 8:

(a) Collisionality The formulation of the lowest moments (26)–(28) of the Boltzmann equation in Section 4 and the transport closure relations mentioned there, was the first step, yielding a system of *two-fluid equations* in terms of the ten variables $n_{e,i}$, $\mathbf{u}_{e,i}$, $T_{e,i}$. To establish the two fluids, the electrons and ions must undergo frequent collisions:

$$\tau_{\rm H} \gg \tau_i \quad \left[\gg \tau_e \right], \tag{56}$$

with $\tau_{\rm H}$ the time scale on which the hydrodynamic description is valid, while τ_e and τ_i indicate the collisional relaxation times of the electrons and ions respectively.

(b) Macroscopic scales Since the two-fluid equations still involves the small length and time scales of the fundamental phenomena we have encountered, viz. the plasma frequency ω_{pe}, the cyclotron frequencies $\Omega_{e,i}$, the Debye length $\lambda_{\rm D}$, and the cyclotron radii $R_{e,i}$, the essential second step towards the *magnetohydrodynamics* (MHD) description of plasmas is to consider *large length and time scales*:

$$\lambda_{\rm MHD} \sim a \gg R_i\,, \qquad \tau_{\rm MHD} \sim a/v_{\rm A} \gg \Omega_i^{-1}\,. \tag{57}$$

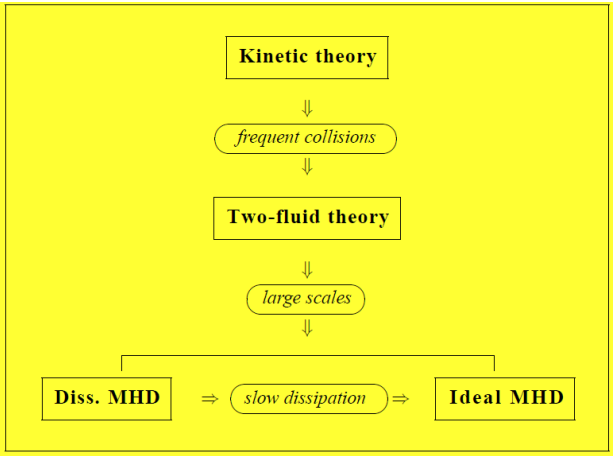

Figure 8: Different theoretical plasma models and their connections. Source Goedbloed, Keppens and Poedts[2].

Hence,the larger the magnetic field strength, the more easy these conditions are satisfied. On these scales, the plasma is considered as a *single* conducting fluid without distinguishing its individual species.

(c) Ideal fluids The third and final step is to consider the plasma dynamics on time scales *faster* than the *slow dissipation* connected with the decay of the macroscopic variables, in particular the resistive decay of the magnetic field:

$$\tau_{\rm MHD} \ll \tau_{\rm R} \sim a^2/\eta\,. \tag{58}$$

This condition is well satisfied for the relatively small sizes of fusion machines, and very easily for the huge sizes of astrophysical plasmas, and leads to the model of *ideal MHD*, which provides a solid macroscopic description of magnetised plasmas.

Acknowledgments

I thank Peter Yoon for kindly providing Figures 4, 5, 6, and 7. These results were obtained in the framework of the projects C14/19/089 (C1 project Internal Funds KU Leuven), G.0D07.19N (FWO-Vlaanderen), SIDC Data Exploitation (ESA Prodex-12), and Belspo projects

BR/165/A2/CCSOM and B2/191/P1/SWiM. For the computations we used the infrastructure of the VSC – Flemish Supercomputer Center, funded by the Hercules foundation and the Flemish Government – department EWI.

References

[1] S.D. Bale, J.C. Kasper, G.G. Howes, E. Quataert, C. Salem, D. Sundkvist, *Phys. Rev. Lett.* **103**, 211101 (2009).

[2] J.P. Goedbloed, R. Keppens and S. Poedts: "Magnetohydrodynamics of laboratory and astrophysical plasmas", Cambridge University Press, 2019. ISBN: 9781107123922

[3] R. Balescu, *Transport Processes in Plasmas; Vol. 1: Classical Transport Theory, Vol. 2: Neoclassical Transport* (Amsterdam, North Holland, 1988).

[4] J. A. Bittencourt, *Fundamentals of Plasma Physics* (New York, Pergamon Press, 1986); 2nd edition (Brazil, Foundation of the State of São Paulo for the Support of Research, 1995).

[5] S. I. Braginskii, 'Transport processes in a plasma', in *Reviews of Plasma Physics, Vol. 1*, ed. M. A. Leontovich (New York, Consultants Bureau, 1965), pp. 205–311.

[6] H. Goldstein, *Classical Mechanics*, 2nd edition (Reading, Addison Wesley, 1980).

[7] F. C. Chen, *Introduction to Plasma Physics and Controlled Fusion, Vol. I: Plasma Physics*, 2nd edition (New York, Plenum Press, 1984).

[8] L. D. Landau, 'The transport equation in the case of Coulomb interactions', *J. Exp. Theor. Phys. USSR* **7** (1937), 203. [Transl.: *Phys. Z. Sowjet.* **10** (1936), 154; or *Collected Papers of L. D. Landau*, ed. D. ter Haar (Oxford, Pergamom Press, 1965) pp. 163–170.]

[9] L. D. Landau, 'On the vibrations of the electronic plasma', *J. Phys. USSR* **10** (1946), 25. [Transl.: *JETP* **16** (1946), 574; or *Collected Papers of L.D. Landau*, ed. D. ter Haar (Oxford, Pergamom Press, 1965) pp. 445–460.]

[10] M. Lazar, V. Pierrard, S.M. Shaaban, H. Fichtner, S. Poedts, 'Dual Maxwellian-Kappa modelling of the solar wind electrons: new clues on the temperature of Kappa populations', *Astron. Astrophys.* **602** (2017), A44.

[11] M. Lazar, S.M. Shaaban, S. Poedts, Š. Štverák, 'Firehose constraints of the bi-Kappa distributed electrons: a zero-order approach for the suprathermal electrons in the solar wind', *Monthly Not. Roy. Astron. Soc.* **464**, 564-571 (2017).

[12] J. H. Malmberg and C. B. Wharton, 'Dispersion of electron plasma waves', *Phys. Rev. Lett.* **17**, 175–178 (1966).

[13] J. H. Malmberg, C. B. Wharton, R. W. Gould and T. M. O'Neil, 'Observation of plasma wave echos', *Phys. Fluids* **11** (1968), 1147–1153.

[14] E. Marsch, R. Schwenn, H. Rosenbauer, K.-H. Muehlhaeuser, W. Pilipp, F.-M. Neubauer, 'Solar wind protons: Three-dimensional velocity distributions and derived plasma parameters measured between 0.3 and 1 AU', *J. Geophys. Res.* **87** (1982), 52-72.

[15] M.J. Michno, M. Lazar, P.H. Yoon, R. Schlickeiser, *Astrophys. J.* **781**, 49 (5pp), 2014.

[16] S.M. Shaaban, M. Lazar, P.H. Yoon, S.Poedts, *Astrophys. J.* **871**, 237 (11pp), 2019.

[17] Š. Štverák, P. Trávníček, M. Maksimovic, E. Marsch, A.N. Fazakerley, E.E. Scime, Journal of Geophysical Research (Space Physics), **113**, A03103 (2008).

[18] N. G. van Kampen, 'On the theory of stationary waves in plasmas', *Physica* **21** (1955), 949–963.

[19] N. G. van Kampen and B. U. Felderhof, *Theoretical Methods in Plasma Physics* (Amsterdam, North-Holland Publishing Company, 1967).

[20] A. A. Vlasov, 'The oscillation properties of an electron gas', *Zhur. Eksp. Teor. Fiz.* **8** (1938), 291–318; 'Vibrational poperties, crystal structure, non-dissipated counterdirected currents and spontaneous origin of these properties in a "gas" ', *J. Phys. USSR* **9** (1945), 25–40.